

Localized, low-voltage electro-osmotic pumping across nanoporous membranes

A. Gupta

Chemical and Biological Engineering Department, Rensselaer Polytechnic Institute, Troy, New York 12180, USA

H. Denver

Mechanical, Aerospace and Nuclear Engineering Department, Rensselaer Polytechnic Institute, Troy, New York 12180, USA

A. H. Hirs

Mechanical, Aerospace and Nuclear Engineering Department, Rensselaer Polytechnic Institute, Troy, New York 12180, USA and Chemical and Biological Engineering Department, Rensselaer Polytechnic Institute, Troy, New York 12180, USA

J. A. Stenken

Department of Chemistry and Chemical Biology, Rensselaer Polytechnic Institute, Troy, New York 12180, USA

D.-A. Borca-Tasciuc^{a)}

Mechanical, Aerospace and Nuclear Engineering Department, Rensselaer Polytechnic Institute, Troy, New York 12180, USA

(Received 11 June 2007; accepted 3 August 2007; published online 28 August 2007)

This work demonstrates the principle of localized, low-voltage, continuous current electro-osmotic pumping across thin membranes. Localization of the pumping effect is obtained by employing ring electrodes, microfabricated on each side of nanoporous alumina membranes. Low voltage actuation is achieved by having the separation of the two electrodes in the microscale range—the thickness of the membrane. The measured electro-osmotic velocity increases linearly from $40 \mu\text{m/s}$ at 5 V to $200 \mu\text{m/s}$ at 20 V . Experimental results compare well with predictions of an electro-osmotic flow model considering the nonuniform distribution of the electric field between the electrodes.

© 2007 American Institute of Physics. [DOI: [10.1063/1.2775836](https://doi.org/10.1063/1.2775836)]

Local pumping/control of minute quantities of liquids is relevant to a variety of applications, including biomedical field and optofluidics. In the field of neuroscience, it is of great interest to determine the spatial distribution of neuro-molecules with high resolution.¹ In the emerging field of optofluidics,² the development of adaptive microlens and reconfigurable photonic crystals are among the current goals.^{3–6} Employing electro-osmotic transport across a porous membrane to achieve local control/pumping of droplets has potential for all of these applications.

Electro-osmosis in porous media is the motion of a liquid relative to the charged walls in the presence of an electric field.⁷ This phenomenon has been traditionally used for wastewater purification, soil decontamination, and bio-separation,^{8–11} though other applications have emerged recently.^{11–13} However, in most of these systems the electrodes used to apply the electric field are placed within the fluid, and the liquid pumping takes place across the entire cross-sectional area of the porous membrane. Due to these constraints, conventional electro-osmotic pumping typically requires large voltages and localized pumping cannot be readily achieved.

The present work demonstrates localized, low-voltage, continuous current (dc) electro-osmotic pumping across a nanoporous alumina membrane. A proof-of-concept device is

shown schematically in Fig. 1. The localized pumping is obtained between thin film, ring electrodes coaxially fabricated on both sides of the membrane. The bottom surface of the membrane is in contact with a liquid reservoir while its top surface is open to the air. When a potential difference is applied to the electrodes, the liquid is pumped from the reservoir through the membrane forming a droplet on its surface at the designated pumping site, as confined by the top electrode.

The porous membranes used in this work are anodic alumina membranes, available commercially (e.g., Whatman Corp.). They have parallel cylindrical pores with a diameter of 200 nm , a porosity of $\sim 50\%$, and a thickness of $\sim 60 \mu\text{m}$ (Fig. 2). The top and bottom ring electrodes were microfabricated through gold sputtering employing a shadow mask

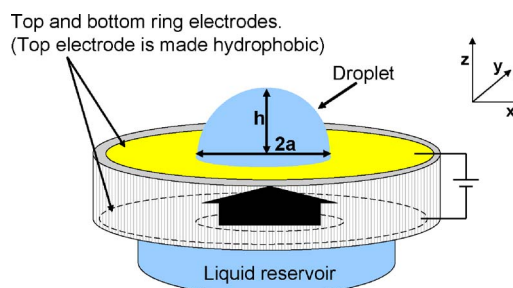


FIG. 1. (Color online) Experimental setup for localized electro-osmotic pumping across nanoporous alumina membrane.

^{a)} Author to whom correspondence should be addressed; electronic mail: borcad@rpi.edu

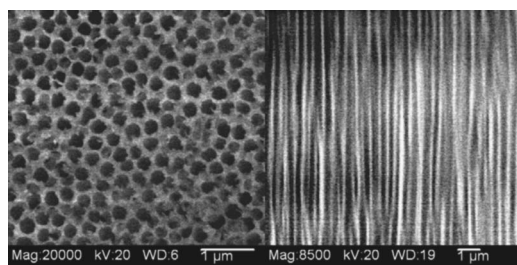


FIG. 2. Scanning electron micrographs of alumina membranes used in present study; (a) top view and (b) cross section.

and connected to the leads from a power supply using 30 μm diameter gold wire. In order to determine the current flow during pumping, a 10 Ω resistor was placed in series with the device and the voltage drop across the resistor was measured. The membrane was placed on top of a liquid reservoir fitted with a refilling channel to compensate for liquid depletion during the experiment. The test liquid was distilled water (Poland Spring) having a pH 6.7, which was filtered through a 200 nm sterile syringe filter from Corning. The liquid volume pumped to the top surface is controlled by the wettability of the gold electrodes to prevent spreading. A solution of 1-octadecanethiol (ODT) in ethanol is applied to the top gold electrode. ODT adheres well to gold,¹⁴ forming a self-assembled monolayer which is strongly hydrophobic. Therefore, the water pumped by electro-osmosis at the center of the device remains at the pumping site (with a radius of 2 mm), where it forms a droplet. The total volume of liquid transferred across the membrane from the reservoir and the flow rate are determined by analyzing digital images of the growing droplet captured at different times using a charge coupled device-video camera. Before the experiment, the sample is primed to ensure that most of the pores are wetted and therefore active (during this time the water pumped at a given actuation voltage is removed with a pipette). A series of digital pictures is subsequently taken at specified time intervals. Afterwards, the applied voltage is changed and the process is repeated. At the end, the magnification ratio of the imaging system is determined via a scale. The images are processed (Vision Assistant Software, National Instruments) to determine the height (h) and the diameter ($2a$) of droplet surface in contact with the membrane (identified in Fig. 1). The volume (v) of the droplet is then calculated as $v = \pi h(a^2 + h^2)/6$. Figure 3 shows an example of the mea-

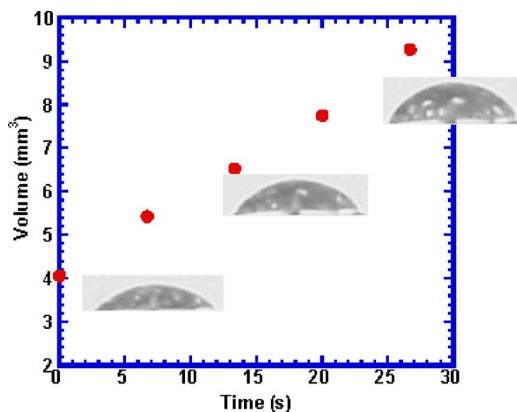


FIG. 3. (Color online) Droplet volume as function of time. The origin of time corresponds to the first picture used for data processing.

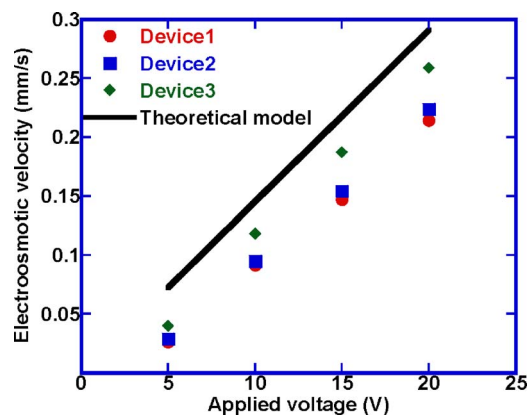


FIG. 4. (Color online) Theoretical (line) and experimental (dots) electroosmotic velocities across nanoporous alumina membrane.

sured volumetric change of a droplet as function of time for an applied potential of 5 V. The volumetric flow rate (\dot{V}) is constant, which is expected as electro-osmotic velocity is constant for a given voltage. The electro-osmotic flow velocity v_{eo} is determined from $v_{eo} = \dot{V}/A_{pores}$, where A_{pores} is the area of all pores in the flow region.

Figure 4 shows the measured electro-osmotic velocities as a function of the applied voltage for three different membranes that exhibited the highest observed flow rates among all tested samples. With the present device configuration, the voltage required to produce electroosmosis is more than an order of magnitude lower than the voltage typically used in electroosmosis applications (in the range of tens to hundreds of volts). For example, at 5 V the electro-osmotic velocity is relatively high at 40 $\mu\text{m/s}$. The significant reduction in the applied voltage required to produce pumping is attributed to the high electric field associated with the small spacing ($\sim 60 \mu\text{m}$) between the two electrodes.

It should be noted that volumetric contribution of oxygen and hydrogen generation due to electrolysis has been neglected when calculating experimental electro-osmotic velocity. The volumetric generation of hydrogen \dot{V}_{H_2} can be estimated based on Faraday's law of electrolysis, assuming ideal gas behavior as,¹² $\dot{V}_{H_2} = IRT/2Fp$, where R is the gas constant, T is the (absolute) temperature, F is Faraday's constant, p is the atmospheric pressure, and I is the electrical current passing through the water. Expectedly, the volumetric oxygen generation is half of that of hydrogen. If gases are trapped in the droplet it may contribute to an increase in its volume. The maximum volumetric contributions from both hydrogen and oxygen are estimated to be $\sim 15\%$ at 5 V and $\sim 6\%$ at 20 V. The generated gas may dissolve into water or may form bubbles that escape to atmosphere. The oxygen and hydrogen solubility in water is $\sim 3\%$ and, respectively, 2% (by volume),¹⁵ hence the maximum volumetric contribution from dissolved gases is less than 5%. However, the bubbles also contribute temporarily to the volume of the droplet. Nevertheless, the total contribution of oxygen and hydrogen (dissolved or bubbles) cannot exceed the ratio estimated based on Faraday's law.

Next, the measured electro-osmotic velocity is compared with theoretical prediction for electro-osmotic flow. The electro-osmotic flow velocity in an open cylindrical channel, in the limit of thin electric double layer is given by¹⁶

$$v_{eo} = \frac{\epsilon_0 \epsilon_r \xi}{\mu} E, \quad (1)$$

where ϵ_0 is vacuum permittivity, ϵ_r is the relative permittivity of the pumped liquid, ξ is Zeta potential associated with the electric double layer, E is the electric field, and μ is the liquid viscosity. The electro-osmotic velocity is calculated assuming the reported value of the Zeta potential as 30 mV (Refs. 17–19) and room temperature values for viscosity. Heating effects were estimated and found negligible in the current experiments (<1 K). Since the electric field between the electrodes is not uniform, an average electric field is evaluated taking into consideration the geometrical configuration of the electrodes. The local electric field due to the two coaxial ring electrodes at a point of coordinates (x, y, z) (Fig. 1) within the pumping area is determined analytically as

$$E(x, y) = \int_{R_{in}}^{R_{out}} \int_0^{2\pi} \frac{\sigma R}{4\pi\epsilon_0\epsilon_r^c [(R \cos \theta - x)^2 + (R \sin \theta - y)^2]^{3/2}} t d\theta dR, \quad (2)$$

where R_{in} and R_{out} are the inner and outer radii, respectively, of the annular electrodes, t is the membrane thickness and, ϵ_r^c is the relative permittivity of the composite media (water and alumina). The charge density σ is calculated as $\sigma = \epsilon \epsilon_r^c V/t$, where V is the voltage applied to the electrode. From Eq. (2) it is observed that the electric field in the membrane is uniform along the z direction due to symmetry of the electrodes. The average electric field can, therefore, be evaluated numerically as $E_{ave} = 1/A \int E(x, y) dA$.

The predicted electro-osmotic velocity is shown with a solid line in Fig. 4. The measured velocity increases linearly with the applied voltage, consistent with the theory. Moreover, the predicted values are in the same range as the measured ones. While the experimentally measured electro-osmotic velocity is only about 50% of the theoretical prediction at 5 V, it reaches almost 90% of the theoretical value at 20 V. There are several factors that can affect the experimental results such as the accuracy of the Zeta potential and presence of clogged pores. An error in Zeta potential cannot explain the decrease in discrepancy with increasing the voltage, since it will change the predicted values by a constant. The effect of clogged pores may, however, be more significant at lower voltages, where the pressure due to electro-osmosis is lower and the flow may not be very efficient in removing potential debris trapped within the pores. It should be noted that several other samples tested exhibited lower flow rates than those reported in Fig 4. The decrease in measured flow rate for these samples is believed to be caused by a reduced number of active pores as result of contamina-

tion, confirming the importance of clogged pores. Although the experiments were performed with great care to minimize contamination, they were carried out in a common laboratory environment. Occasionally, particles larger in size than the pores' diameter may have come in contact with the membrane surface blocking the transport of water through some of the pores during the experiments. In addition, for some of the samples tested, the ODT coating was observed to cause a decrease in flow rate, possible due to clogged pores in the pumping area.

The electro-osmotic approach to transport liquid droplets onto and off a surface may have applications in a wide range of industries from optoelectronics and manufacturing to clinical testing and diagnostics. Furthermore, since the power dissipated by the current device is relatively low, ranging from 625 μ W to 8 mW, this approach may be of particular interest for portable electronics applications where power consumption is critical.

- ¹J. L. Peters and A. C. Michael, *J. Neurochem.* **74**, 1563 (2000).
- ²D. Psaltis, S. R. Quake, and, C. Yang, *Nature (London)* **442**, 381 (2006).
- ³L. Dong, A. K. Agarwal, D. J. Beebe, and H. Jiang, *Nature (London)* **442**, 551 (2006).
- ⁴C. A. Lopez, Chin-Chen Lee, and A. H. Hirsra, *Appl. Phys. Lett.* **87**, 134102 (2005).
- ⁵S. Kuiper and B. H. W. Hendriks, *Appl. Phys. Lett.* **85**, 1128 (2004).
- ⁶D. Erickson, T. Rockwood, T. Emery, A. Scherer, and D. Psaltis, *Opt. Lett.* **31**, 59 (2006).
- ⁷R. F. Probst, *Physicochemical Hydrodynamics: An Introduction* (Butterworth, Stoneham, MA, 1989), p. 191.
- ⁸R. F. Probst and R. E. Hicks, *Science* **260**, 498 (1993).
- ⁹I. Gingerich, R. Neufeld, and T. Thomas, *Water Environ. Res.* **71**, 267 (1999).
- ¹⁰S. Ghosal, *Annu. Rev. Fluid Mech.* **38**, 309 (2006).
- ¹¹M. J. Vogel, P. Ehrhard, and P. H. Steen, *Proc. Natl. Acad. Sci. U.S.A.* **102**, 11974 (2005).
- ¹²P. Prakash, M. D. Grissom, C. D. Rahn, and A. L. Zydney, *J. Membr. Sci.* **286**, 153 (2006).
- ¹³J. G. Santiago, C. R. Buie, J. D. Posner, T. Fabian, S.-W. Cha, D. Kim, F. B. Prinz, and J. K. Eaton, *J. Power Sources* **161**, 191 (2006).
- ¹⁴M. Geissler, P. Chalsani, N. S. Cameron, and T. Veres, *Small* **6**, 760 (2006).
- ¹⁵*Perry's Chemical Engineers' Handbook*, 7th ed., edited by R. H. Perry and D. W. Green (McGraw-Hill, New York, 2001), pp. 2–126.
- ¹⁶C. L. Rice and R. Whitehead, *J. Phys. Chem.* **69**, 4017 (1965).
- ¹⁷T. Gopal and J. B. Talbot, *J. Electrochem. Soc.* **153**, G622 (2006).
- ¹⁸L. Palmqvist, O. Lyckfeldt, E. Carlstrom, P. Davoust, A. Kauppi, and K. Holmberg, *Colloids Surf., A* **274**, 100 (2006).
- ¹⁹Zeta potential depends on both pH and ionic strength of the pumped liquid. However an order of magnitude increase in ionic strength, from 1 mM KNO₃ (Ref. 17) to 0.01M KCl (Ref. 18), results in a relatively small change in Zeta potential from ~25 to ~35 mV at a pH ~6.7—the pH of distilled water used in present experiment. The ionic strength of water used is not known; however, it is expected to be relatively low.